Effect of Step Layer Width and Electric Field on Single-Particle States in Step Quantum Well Structures

Piyawong Poopanya[1], Natthakan Rueangnetr[2], Worachet Bukaew[2] and Kanchana Sivalertporn[2]*

[1]Program of Physics, Faculty of Science, Ubon Ratchathani Rajabhat University, Ubon Ratchathani, 34000, Thailand

[2]Department of Physics, Faculty of Science, Ubon Ratchathani University, Ubon Ratchathani, 34190, Thailand

* Corresponding author. E-mail address: kanchana.s@ubu.ac.th

Abstract

The single-particle states in AlGaAs/GaAs and GaInNAs/GaAs step quantum well structures have been theoretically studied by solving straight-forwardly the Schrodinger equation in real space. The electron and hole energy levels were calculated for different well widths and step layer widths. It was found that the energies are decreased with increasing the well width and step layer width, but the change is very small for a wide layer. There are two states with few meV energy splitting observed at the energy a bit above the step potential. Therefore, these two levels can be controlled by varying the step potential. The electron and hole energies in AlGaAs/GaAs and GaInNAs/GaAs step quantum well structures were compared to that in the single squared quantum well. The results showed that the energies decrease with the same trend and comparable percentage for both electron and hole cases. The ground state energy can be decreased up to nearly 50% for the step layer of 10 nm at small well width. The electron and hole energies were also calculated for applied electric fields up to 200 kV/cm. The tilted potential due to the electric field results in the localization of electron and hole in the different layer and breaks the symmetry of their wave functions. At a large enough field, the ground-state electron (hole) is confined in the left (right) step layer which corresponds to the anticrossing at around 130 kV/cm for electron and 70 kV/cm for hole in the field dependence of energy profile.

Keywords: step quantum wells, step-layer width, single-particle state

Introduction

The semiconductor quantum well (QW) heterostructures have been attracted much attention for few decades due to their potential applications in optoelectronic devices such as laser diodes (Dehimi, Dehimi, Asar, Mebarki, & Zelik, 2017), photodetectors (Albo, Fekete, & Bahir, 2019), solar cell (Urabe et al., 2015; Khalil et al., 2012), and microcavity (Sivalertporn & Muljarov, 2015; Wilkes & Muljarov, 2016). The electronic and optical properties can be controlled by varying the well width, potential height or external electric field applied in the growth direction. Therefore, the effect of these parameters on electron, hole and exciton states have been theoretically investigated in order to improve the device efficiency (Poopanya & Sivalertporn, 2018; Sivalertporn, 2016; Ozturk, Ozturk, & Elagoz, 2018; Gu et al., 2017; Miyoshi, Tsutsumi, Kabata, Mori, & Egawa, 2017; Grigoryev et al., 2016; Dietrich et al., 2015). The conversion efficiency of GaN/InGaN multi quantum well (MQW) solar cell have been calculated for different structural parameters such as thickness, potential and number of QW layers. The results can be used to design and interpret the characteristic of optimized MQW solar cell (Mahala, Singh, & Dhanavantri, 2018). The optical properties of InGaN laser diodes have been studied for different well thickness to obtain the best design for laser diode (Abdullah & Ibrahim, 2013). It was found that the optical gain is large if a QW thickness is small because the carriers are confined and localized in a small QW. A double QW consisting of two QWs separated by a thin barrier layer is a interesting structure. The reason is that the indirect exciton (an electron and a hole are in different well) can be formed when the electric field is applied

in such structure (Sivalertporn, Mouchliadis, Ivanov, Philp, & Muljarov, 2012; Ungan et al., 2013; Yesilgul et al., 2016). The indirect exciton has a longer lifetime and larger binding energy compared to the direct exciton in a single QW structure (Alexandrou et al., 1990). Recently, it has been reported that the spin relaxation time of indirect exciton is 100 times larger than that of direct exciton (Andreakou et al., 2015). Not only the square well, but the shape of potential profile is also a significant parameter. Different shapes give rise to different electronic property of the device (Ryczko & Sek, 2019; Kasapoglu et al., 2015; Zhang, Zou, Liu, & Yuan, 2015). In this work, we concentrate on AlGaAs/GaAs and GaInNAs/GaAs step QW structures in order to study the effect of step layer on the electron and hole states. The former structure is used in various electronics and photoelectronic devices, while the latter structure has been attracting great interest due to their direct and large band gap which is appropriate for short wavelength devices. The dilute nitride III-V compound semiconductor has a wide range of band gap varied from 0.64 eV (InN) to 3.4 eV (GaN). Therefore, it is suitable for solar cell applications as well.

Theoretical Model

Let us consider a symmetric QW structure consisting of a QW layers sandwiched between two step layers with the width L_t. The system is surrounded on both sides by thick barriers with wider band gap (Figure 1). The step potential V_1 is set to be lower than the surrounded potential V to make a step-like QW.

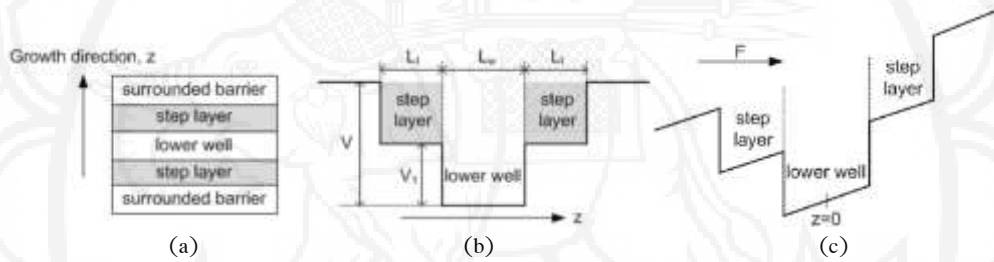| (a) | (b) | (c) |

Figure 1 Step QW structure: (a) cross section of QW structure, (b)-(c) schematic band diagram of QW in the absence and presence of applied electric field (F), respectively

Under the effective mass approximation, the electron and hole eigen energies are calculated by solving the Schrodinger equation:

$$\left(-\frac{\hbar^2}{2}\frac{\partial}{\partial z}\frac{1}{m}\frac{\partial}{\partial z} + V_{e(h)}(z) \right)\varphi_{e(h)} = E_{e(h)}\varphi_{e(h)} \tag{1}$$

where $E_{e(h)}$ is the electron (hole) energy, z is the electron/hole coordinate in the growth direction, $m_{e(h)}$ is the electron (hole) effective mass and $V_{e(h)}$ is the electron (hole) confinement potential which has a step-like profile:

$$V_{e(h)}(z) = \begin{cases} 0, & |z| \leq L_w/2 \\ V_{1,e(h)}, & L_w/2 \leq |z| \leq L_w/2 + L_t \\ V_{e(h)}, & |z| \geq L_w/2 + L_t \end{cases} \tag{2}$$

The single-particle wave functions $\varphi_{e(h)}(z)$ satisfying the Schrodinger equation is a combination of two exponential terms (incoming and outgoing parts). In the presence of electric field, the Schrodinger equation is given by

$$\left(-\frac{\hbar^2}{2}\frac{\partial}{\partial z}\frac{1}{m}\frac{\partial}{\partial z}+V_{e(h)}(z)\pm eFz\right)\varphi=E_{e(h)}\varphi_{e(h)}, \tag{3}$$

The solution of Eq. (3) is the combination of Airy functions:

$$\varphi(\xi)=aAi(\xi)+bBi(\xi), \tag{4}$$

where a and b are an arbitrary constant, and $\xi=\left(2mF/\hbar^2\right)^{1/3}\left(z+(V-E)/F\right)$. For five regions of the step QW, we have five pairs of unknown coefficients (a_i, b_i). The outgoing wave at $z\to-\infty$ (for electron) yields $b_1=-ia_1$ and $b_5=0$ since no electron can escape to the other side ($z\to+\infty$). Therefore, we now have only eight unknown coefficients and the eigenvalue which can be calculated from the eight equations of boundary conditions at heterostructure interfaces including the continuity of wave functions and their derivatives. The normalization condition of the wave function $\int_{-\infty}^{\infty}\left|\varphi_{e(h)}\right|^2 dz=1$ was also applied to find the unknown coefficients. The wave function is then calculated from the obtained eigen energy and coefficients. Changing the structural parameters results in the change of eigen energy and coefficients (a_i, b_i). The detail of the model is explained in our previous work (Sivalertporn et al., 2012).

Results and Discussion

We consider $Al_xGa_{1-x}As/GaAs$ (with x=0.33) and $Ga_{1-x}In_xN_yAs_{1-y}/GaAs$ (with x=0.35, y=0.005) step QW structures. A QW layer has narrow band gap, while a wider band gap material is used as a surrounded barrier. The step layer material is the same material as the surrounded layer but has different x and y contents. The parameters for the step layer were calculated by linear interpolation between the well layer and barrier layer. The well width and step layer width were varied from 0.1 nm to 12 nm. The parameters for electron/hole mass and potential are shown in Table 1. The mass m_1, m_2 and m_3 are the mass in well layer, barrier layer and step layer respectively. The effect of well width, step layer width, potential height and applied electric field on the electron and hole states have been studied. The results are shown as the following.

Table 1 Parameters used in the calculation

parameter	AlGaAs/GaAs (Sivalertporn et al., 2016)	GaInNAs/GaAs (Yesilgul, Ungan, Kasapoglu, Sari, & Sokmen, 2012)
V_e (meV)	267.48	438.83
V_h (meV)	144.03	109.70
Well layer	GaAs	GaInNAs
$m_{1,e}(m_0)$	0.0665	0.0656
$m_{1,h}(m_0)$	0.34	0.3447
barrier layer	AlGaAs	GaAs
$m_{2,e}(m_0)$	0.0941	0.0665
$m_{2,h}(m_0)$	0.476	0.34

1. Structure Dependence

The electron and hole energies in AlGaAs/GaAs step QW structure with different step layer widths were calculated as a function of well width (Figure 2). The energies for all cases are decreased with increasing the well width. Adding the step layer gives rise to the decrease of electron and hole energies compared to the single squared well structure. For the ground state (GS), the energy of electron (hole) rapidly drops from 265 meV (142 meV) in single squared well to 200 meV (90 meV) in the case of 2-nm step layer. However, the energy changes very small when the step layer is increased from 6-nm to 10-nm.

It is clearly seen from Figure 2(a) and Figure 2(c) that the electron and hole energies in 10-nm step QW are very close to that of 6-nm step layer case. Only a small difference is observed at a narrow well width. The reason is that all these energies are lower than the step potential ($V_{1,e}$=133.74 meV for electron and $V_{1,h}$=72.02 meV for hole) residing in the lower QW, so that the change of step layer width does not affect to these energy levels. At approximately L_w=6nm (L_w=2 nm), the electron (hole) energies in step QW for all cases are the same at the energy of around 60 meV (40 meV). It is observed at a narrower well in the case of hole because of the heavier mass and lower potential of hole. For the first excited state (1st ES) [Figure 2(b) and 2(d)], it is also observed a large difference in energy between 2-nm and 6-nm cases and only a small change between 6-nm and 10-nm of step layer. Again, when the energies are lower than the potential V_1 means that the state already occupies in the lower well. The step layer has no longer influence on the energy and all levels tend to the same level.
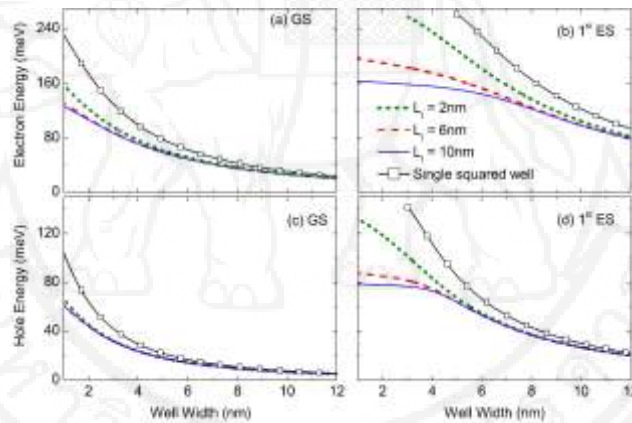

Figure 2 Ground state (GS) and the first excited state (1st ES) energies in AlGaAs/GaAs step QW structure as a function of well width for L_t=2 nm (solid), 6 nm (dashed) and 10 nm (dotted)
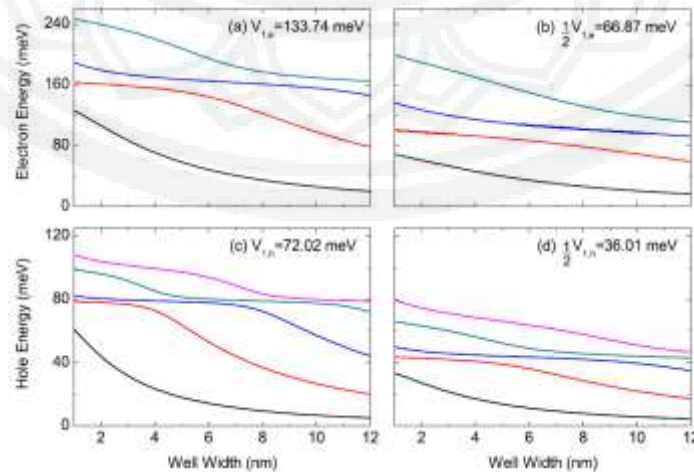

Figure 3 Four electron states and five hole states in AlGaAs/GaAs step QW structure for L_t=10 nm

Figure 3 shows the electron and hole energies in a 10-nm step QW structure (four states of electron and five states of hole). Noted that there are excited states lie parallel at the energy of approximately 160 meV for electron and 80 meV for hole which are near the bottom of the step potential. The hole energy in Figure 3(c) shows that the first excited state energy remains unchange at 80 meV at $L_w=1$ nm, while the second excited state starts at around 95 meV and decreases to 80 meV. The second excited state then remains at this level and parallel to the first excited state for $L_w<4$ nm. When $L_w>4$ nm the first excited state drops down to lower energy, the third excited state comes to the level of 80 meV and is parallel to the second excited state for the well width of $L_w=5-8$ meV. The same also happens for the fourth excited state and so on. The energy splitting of two paralleling states is about 10 meV for electron and 3 meV for hole. The step potential V_1 is decreased by a factor of two in order to see how the electron and hole energies change [Figure. 3(b) and 3(d)]. It was found that the energy trend does not change, the calculated energies only shift down to lower energy due to a lower potential. There also be two paralleling energy levels at the energy which is above the step potential $V_1/2$. The splitting between the two energies is twice compared to the case of V_1 step potential. The hole wave functions of five states in AlGaAs/GaAs step QW structure are demonstrated in Figure 4. The white dashed lines indicate the region inside the lower well, while the while dotted lines show the edge of the step layer. It was found that there are two broadening peaks in the step well region when the excited state remains at the parallel level ($L_w<4$ nm for 1st ES, $L_w<8$ nm for 2nd ES, $4<L_w<11$ nm for 3rd ES, $L_w>8$ nm for 4th ES). As we know, the Nth excited state should have N maxima of the wave function. However, all peaks in the middle always very small compared to the two broadening peaks. The sharp peaks inside the well region in Figure 4(b) for $L_w>4$ nm and in Figure 4(c) for $L_w>8$ nm are observed when hole energy drops down to the level below the step potential, corresponding to a strongly decrease of energy as the well width increases in Figure 3.
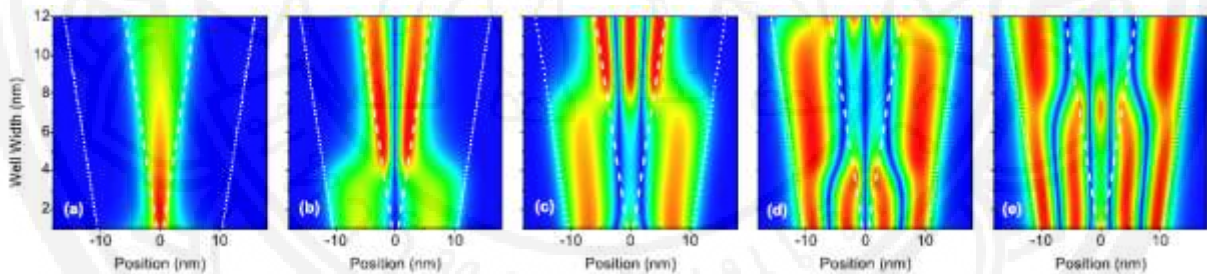

Figure 4 Hole wave functions in AlGaAs/GaAs step QW structure for $L_t=10$ nm: (a) GS, (b) 1st ES, (c) 2nd ES, (d) 3rd ES, and (e) 4th ES states. The region inside two white dashed lines is the lower well region, while two white dotted lines indicate the step layer edges
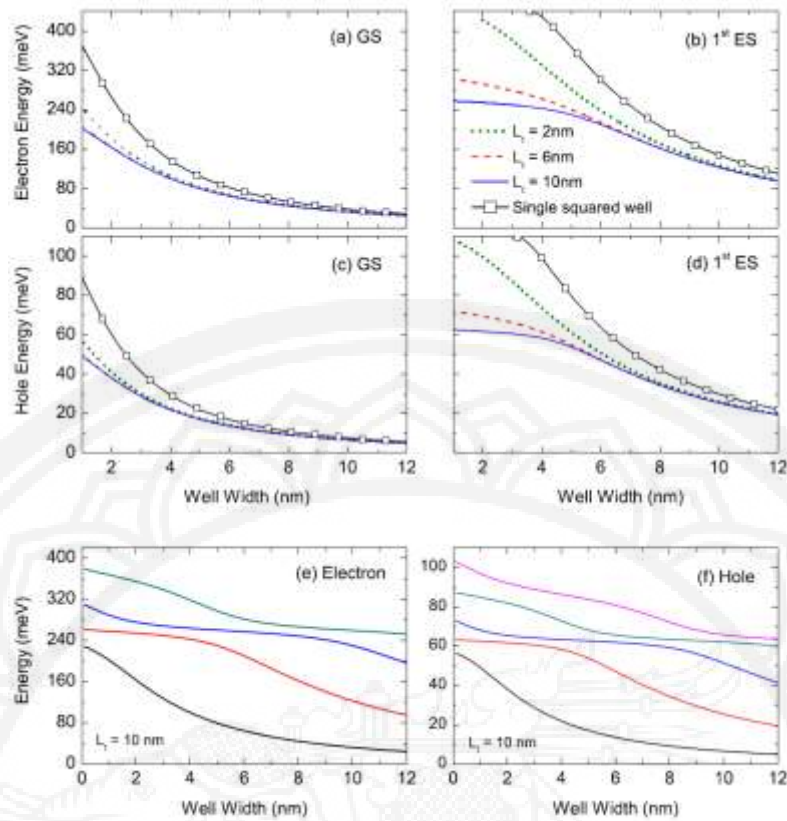
Figure 5 Ground state (GS) and the first excited state (1ˢᵗ ES) energies in GaInNAs/GaAs step QW structure as a function of well width for L_t=2 nm (solid), 6 nm (dashed) and 10 nm (dotted)
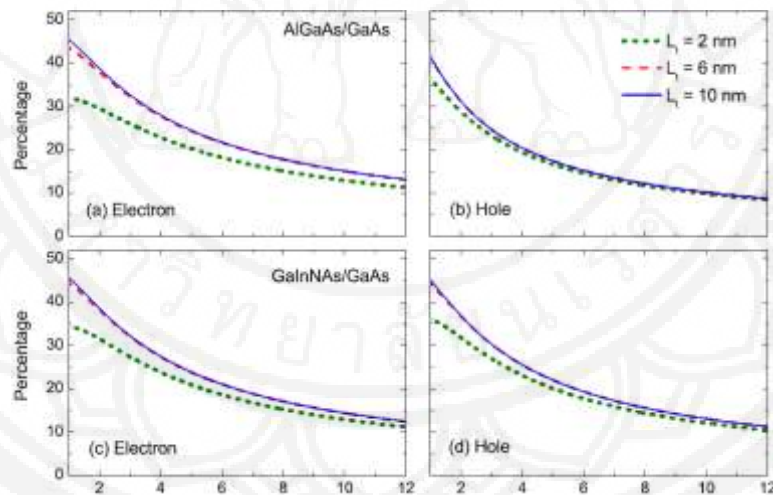

Figure 6 Percentage of ground state energy difference between the step QW and single squared QW for (a)-(b) AlGaAs/GaAs and (c)-(d) GaInNAs/GaAs structures

We have also calculated the electron and hole energies in the GaInNAs step QW structure (Figure 5). The parameters used in the calculation are shown in Table 1. The results showed that the well width dependence of energies looks very similar to those in AlGaAs/GaAs step QW structure. In order to understand in more details, we have calculated the difference of electron and hole energies in the step QW (E_{step}) compared to their energies in the single squared QW ($E_{squared}$) and calculate their percentage by

$$\Delta E = E_{squared} - E_{step}, \tag{6}$$

$$\%E = \frac{\Delta E}{E_{squared}} \times 100, \tag{7}$$

Figure 6 shows the decreasing rate of ground state energy in AlGaAs／GaAs and GaInNAs／GaAs step QW structures as a function of well width. The percentages of energy difference exhibit the similar trend for both electron and hole. The ground state energy can be reduced up to nearly 50％ for 10-nm step layer width and a narrow well width. For a wider well width, the decreasing rates are saturated at about 10％ for all values of step layer. This is because the step layer width does not influence on the ground state energy as discussed before.

2. Electric field dependence

When the electric field is applied to the structure in the growth direction, the potential profile is tilted as shown in Figure 1(c). The electron and hole energies were calculated for the electric field (F) up to 200 kV／cm and the step layer width was fixed at L_t=10 nm. The results showed that the ground state energy remains nearly constant at low electric field and the energies then linearly are decreased with increasing field giving rise to an anticrossing in energy (Figure 7). This anticrossing happens at larger field for wider well width. The first four energy states of electron and hole for L_t= 8 nm are demonstrated in Figure 7(c)-(d). The anticrossing of GS-1st ES energy happens at around F=130 kV／cm for electron and F=75 kV／cm for hole. The electron wave functions at F=120 kV／cm (before the electron anticrossing) and F=140 kV／cm (after the electron anticrossing) in Figure 7(e) show that the maximum of the wave function changes from the well layer to step layer. The reason why electron is now confined in the step layer after the anticrossing is because the large field makes the step layer potential becomes lower than the well potential. Moreover, the tilted potential due to the electric field can cause the tunneling of electron／hole through the surrounded barrier which can be observed the oscillation in the left region as shown in Figure 7(e). A larger field leads to a larger tunneling effect.
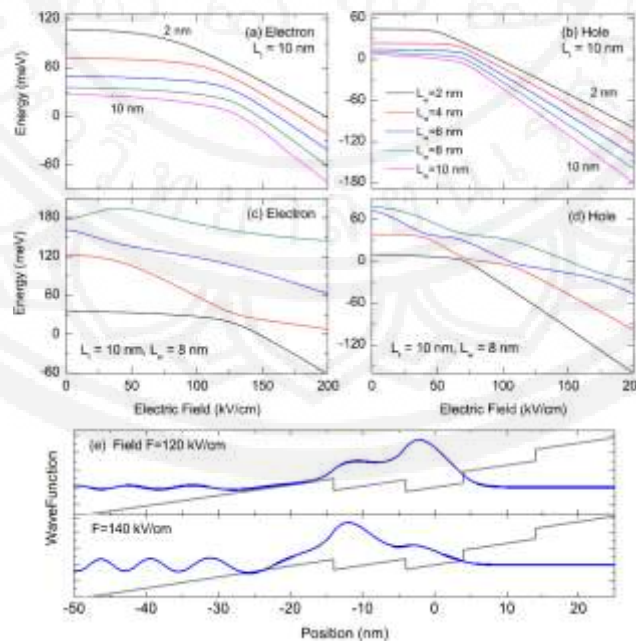

Figure 7 Electric field dependence of electron and hole energy in AlGaAs/GaAs step QW structure: (a)-(b) showing the GS energy for different step layer widths L_t, (c)-(d) demonstrating four energy levels for L_t= 10 nm and L_w= 8 nm. The wave functions of electron ground state at F=120 kV／cm and F=140 kV／cm are demonstrated in (e)
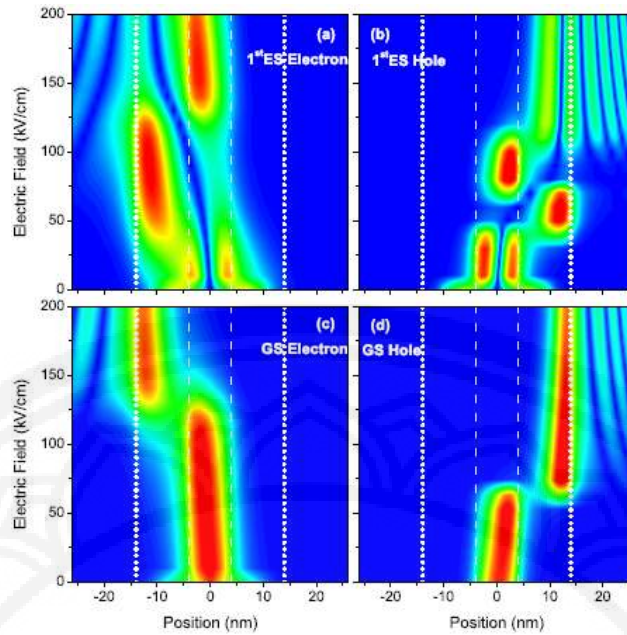
Figure 8 Wave functions of electron and hole in AlGaAs/GaAs step QW structure for $L_t = 10$ nm and $L_w = 8$ nm. The region inside two dashed lines is the lower well region, while dotted lines indicate the step layer edges

The electron and hole wave functions for $L_t = 10$ nm and $L_w = 8$ nm are plotted as a function of electric field (Figure 8). Electron and hole ground states are not confined at the center anymore. Electron moves to the left and hole moves to the right due to the electric field. The wave function maxima of electron (hole) are observed at the left (right) wall. The change of wave function localization occurs at the energy anticrossing. After the anticrossing, the ground state electron locates in the left step layer, while the first excited state electron is confined in the well layer instead. The same situation also happens in the case of hole, but hole will move to the right. Note that ground state electron is in the left step layer and ground state hole resides in the right step layer at large field, so that it is possible to form an indirect exciton in the step QW structure.

Conclusion

The electron and hole energies and wave functions in step QW structures have been calculated for different well width and step layer width. We consider AlGaAs/GaAs and GaInNAs/GaAs structures in order to study the effect of mass and potential height on electron and hole energies. Due to the quantum confinement effect, the electron and hole energy levels are discrete and exhibit the blue shift in energy as the width is decreased. The narrower the well width, the higher the energy. It was found that the energies in AlGaAs/ GaAs and GaInNAs/GaAs step QWs decrease with comparable percentage compared to their own single squared well level. The trends for electron and hole are similar. This means that we can predict the electron and hole energies in any step QWs from their single QW structures. With no electric field, the wave functions are symmetric and the probability of finding ground state electron (hole) is highest at the center of the well. The well width dependence of energy shows the two excited state energies lie parallel to each other at the energy near a bottom of step layer. The wave function of these two states has its maxima at the center of step layers with a broadening peak.

In the presence of the electric field, the symmetry of the system is broken and the potential is tilted. As a result, electron move to the left and hole move to the right due to the field creating an indirect exciton. The GS-

1st ES anticrossing happens when the electric field is large enough to make the step potential is lower than the well potential. The GS electron (hole) after the anticrossing is confined in a left (right) step layer, while the 1st ES electron (hole) localization changes from a left (right) step layer to well layer. Finally, it can be concluded that the model can be used to studied the electron and hole states in the step QW structure for various structure parameters. The obtained results for single-particle state can then be used to calculate the exciton states and their properties which plays a significant role in the optoelectronic applications. The modelling predictions are a useful guide for experiments to understand background physics and design the optimized devices.

Acknowledgments

References

Abdullah, R. A., & Ibrahim, K. (2013). Effects of quantum confined stark effect and well thickness on optical properties of double quantum wells violet InGaN laser diodes. *Optik*, *124*(4), 292-296.

Albo, A., Fekete, D., & Bahir, G. (2019). The opportunity of using InGaAsN/AlGaAs quantum wells forextended short-wavelength infrared photodetection. *Infrared Physics & Technology*, *96,* 68-76.

Alexandrou, A., Kash, J. A., Mendez, E. E., Zachau, M., Hong, J. M., Fukuzawa, T., & Hase, Y. (1990). Electric-field effects on exciton lifetimes in symmetric coupled GaAs/Al$_{0.3}$Ga$_{0.7}$As double quantum wells. *Physical Review B*, *42*(14), 9225-9228.

Andreakou, P., Cronenberger, S., Scalbert, D., Nalitov, A., Gippius, N. A., Kavokin, A. V., … Vladimirova, M. (2015). Nonlinear optical spectroscopy of indirect excitons in coupled quantum wells. *Physical Review B*, *91*(12), 125437.

Dehimi, S., Dehimi, L., Asar, T., Mebarki, B., & Zelik, S. (2017). Modeling and simulation of Zn$_x$Cd$_{1-x}$Te/ZnTe quantum well structure for laser applications. *Optik*, *135,* 153-159.

Dietrich, S., Kanter, J., Mayer, W., Vitkalov, S., Dmitriev, D. V., & Bykov, A. A. (2015). Quantum electron lifetime in GaAs quantum wells with three populated subbands. *Physical Review B*, *92*(15), 155411.

Grigoryev, P. S., Kurdyubov, A. S., Kuznetsova, M. S., Ignatiev, I. V., Efimov, Y. P., Eliseev, S. A., … Shapochkin, P. Y. (2016). Excitons in asymmetric quantum wells. *Superlattices and Microstructures*, *97,* 452-462.

Gu, Z., Zhu, Z. N., Wang, M. M., Wang, Y. Q., Wang, M. S., Qu, Y., & Ban, S. L. (2017). Interband optical absorption in wurtzite Mg$_x$Zn$_{1-x}$O/ZnO/Mg$_y$Zn$_{1-y}$O asymmetric quantum wells. *Superlattices and Microstructures*, *102,* 391-398.

Kasapoglu, E., Duque, C. A., Mora-Ramos, M. E., Restrepo, R. L., Ungan, F., Yesilgul, U., ... Sari, H. (2015). Combined effects of intense laser field, electric and magnetic fields on the nonlinear optical properties of the step-like quantum well. *Materials Chemistry and Physics*, *154,* 170-175.

Khalil, H. M., Mazzucato, S., Ardali, S., Celik, O., Mutlu, S., Royall, B., ... Guina, M. (2012). Temperature and magnetic field effect on oscillations observed in GaInNAs/GaAs multiple quantum wells structures. *Materials Science and Engineering*: B, *177*(10), 729-733.

Mahala, P., Singh, S., & Dhanavantri, C. (2018). Design optimization of multi quantum well solar cells. *Optik*, *166,* 61-68.

Miyoshi, M., Tsutsumi, T., Kabata, T., Mori, T., & Egawa, T. (2017). Effect of well layer thickness on quantum and energy conversion efficiencies for InGaN/GaN multiple quantum well solar cells. *Solid-State Electronics*, *129,* 29-34.

Ozturk, O., Ozturk, E., & Elagoz, S. (2018). The effect of barrier width on the electronic properties of double GaAlAs/GaAs and GaInAs/GaAs quantum wells. *Journal of Molecular Structure*, *1156,* 726-732.

Poopanya, P., & Sivalertporn, K. (2018). Exciton states in asymmetric GaInNAs/GaAs coupled quantum wells in an applied electric field. *Physics Letters A*, *382*(10), 734-738.

Ryczko, K., & Sek, G. (2019). M-shaped quantum wells for active region of interband cascade laser. *Optical Materials*, *88,* 252-255.

Sivalertporn, K. (2016). Effect of barrier width on the exciton states in coupled quantum wells in an applied electric field. *Physics Letters A*, *380*(22-23), 1990-1994.

Sivalertporn, K., & Muljarov, E. A. (2015). Controlled strong coupling and absence of dark polaritons in microcavities with double quantum wells. *Physical Review Letters*, *115*(7), 077401.

Sivalertporn, K., Mouchliadis, L., Ivanov, A. L., Philp, R., & Muljarov, E. A. (2012). Direct and indirect excitons in semiconductor coupled quantum wells in an applied electric field. *Physical Review B*, *85*(4), 045207.

Ungan, F., Yesilgul, U., Sakiroglu, S., Kasapoglu, E., Sari, H., Sokmen, I., & Lumin, J. (2013). Nonlinear optical absorption and refractive index in GaInNAs/GaAs double quantum wells under intense laser field and applied electric field. *Journal of Luminescence*, *143,* 75-80.

Urabe, H., Kuramoto, M., Nakano, T., Kawaharazuka, A., Makimoto, T., & Horikoshi, Y. (2015). Effects of surface barrier layer in AlGaAs/GaAs solar cells. *Journal of Crystal Growth*, *425,* 330-332.

Wilkes, J., & Muljarov, E. A. (2016). Dipolar polaritons in microcavity-embedded coupled quantum wells in electric and magnetic fields. *Physical Review B*, *94*(12), 125310.

Yesilgul, U., Ali, E. B., Martinez-Orozco, J. C., Restrepo, R. L., Mora-Ramos, M. E., Duque, C. A., ... Kasapoglu, E. (2016). Linear and nonlinear optical properties in an asymmetric double quantum well under intense laser field: Effects of applied electric and magnetic fields. *Optical Materials*, *58,* 107-112.

Yesilgul, U., Ungan, F., Kasapoglu, E., Sari, H., & Sokmen, I. (2012). Effects of an intense, high-frequency laser field on the binding energy of excitons confined in a GaInNAs/GaAs quantum well. *Physica B: Condensed Matter*, *407,* 528.

Zhang, Z.-H., Zou, L., Liu, C., & Yuan, J.-H. (2015). Electric field effect on the nonlinear optical properties in asymmetrical Gaussian potential quantum wells. *Superlattices and Microstructures*, *85,* 385-391.